論文 / 著書情報
Article / Book Information

論題(和文)	
Title(English)	Influence of Sensor Configuration on Wind Estimation by Equivalent-Input-Disturbance Method for Nonlinear Systems
著者(和文)	RAZELLE DENNISE SORIANO, 佐藤大樹, 宮本皓, 陳引力, 佘錦華
Authors(English)	Razelle Dennise Agoba Soriano, Daiki Sato, Kou Miyamoto, Yinli Chen, Jinhua She
出典(和文)	日本建築学会大会学術講演梗概集, 構造II, , pp. 1019-1020
Citation(English)	, 構造II, , pp. 1019-1020
発行日 / Pub. date	2025, 9
権利情報	一般社団法人 日本建築学会

Influence of Sensor Configuration on Wind Estimation by Equivalent-Input-Disturbance Method for Nonlinear Systems

正会員 ○ SORIANO Razelle Dennise *1　同 佐藤 大樹*1
同 宮本 皓*2　同 陳 引力*1
同 佘 錦華*3

Wind force estimation　Base-isolation　Nonlinear model
Wind force responses　EID Method　Cubic spline interpolation

1. Introduction

Tall base-isolated buildings subjected to strong wind forces are at risk of their isolation layer exceeding its elastic limits, requiring time-history analysis to capture the nonlinear dynamic response accurately. A critical element of such analysis is the estimation of wind forces acting on the structure. Traditional methods, such as wind tunnel tests and CFD simulations, rely on probabilistic assumptions that may introduce uncertainties. An alternative approach, based on She et al. [1] is to use structural response data from monitoring systems to estimate the wind forces by performing the Equivalent-Input-Disturbance method for Nonlinear Systems (EID-NS). The accuracy of the EID-NS method, however, is highly dependent on the number and placement of sensors, as an insufficient number of response measurements can lead to inaccurate force estimations. This paper investigates the impact of various sensor configurations on wind force estimation in nonlinear base-isolated buildings, aiming to identify an optimal sensor setup that ensures high accuracy while remaining practical for real-world implementation.

2. Theoretical Background

2.1. Response Identification

In practical structural monitoring, the number of available accelerometers is often limited, and therefore, only acceleration responses at specific locations are directly measurable. For the purpose of this study, it is assumed that accelerometers are installed at a limited number of locations within the structure. In prior applications of the EID method in wind force estimation [2, 3], the velocity response was typically assumed to be known. However, in most real-world scenarios, acceleration responses are the primary measurements obtained.

To address this, it is assumed that acceleration responses are available only at the specified sensor locations. For the unmeasured stories, the acceleration response is estimated using cubic spline interpolation. These estimated accelerations are then integrated to obtain the corresponding velocity response. Subsequently, the velocity response is utilized within the EID-NS method to estimate the wind forces acting on the structure.

2.2. Wind Force Estimation by EID Method

The estimation of wind forces by EID and EID-NS method, as applied in [2,3], is based on the equation of motion for a system subjected to external wind forces, $\{F(t)\}$:

$$M_s\ddot{x}(t) + C_s\dot{x}(t) + K_s x(t) = E_d F(t) \tag{1}$$

where M_s, C_s, and K_s are the property matrices, namely, mass, damping, and stiffness, respectively. The acceleration, velocity, and displacement responses are given by $\{\ddot{x}(t)\}$, $\{\dot{x}(t)\}$, and $\{x(t)\}$, respectively. E_d is the force-input channel. The state space representation of the system is given by:

$$\begin{cases} \dot{z}(t) = Az(t) + B_d d(t) \\ y(t) = Cz(t) \end{cases} \tag{2}$$

$$\begin{cases} A = \begin{bmatrix} 0 & I_N \\ -{M_s}^{-1}K_s & -{M_s}^{-1}C_s \end{bmatrix} & B_d = \begin{bmatrix} 0 \\ -{M_s}^{-1}E_d \end{bmatrix} \\ d(t) = F(t) & z(t) = \begin{bmatrix} x(t) \\ \dot{x}(t) \end{bmatrix} \end{cases} \tag{3}$$

where A is the system matrix, B_d is the disturbance input matrix, $d(t)$ is the disturbance or the wind force, and $z(t)$ represents the states of the system. The output matrix, C indicates the availability of the states and $y(t)$ is the output of the system. The full state observer of Eq. (2) is given by:

$$\begin{cases} \dot{\hat{z}}(t) = A\hat{z}(t) + LC\,[z(t) - \hat{z}(t)] \\ \hat{y}(t) = C\hat{z}(t) \end{cases} \tag{4}$$

where $\hat{z}(t)$ is an estimated $z(t)$ and L is the observer gain, calculated using the Linear Quadratic Regulator (LQR). The equivalent-input disturbance, $\hat{d}_e(t)$ is determined by:

$$\begin{cases} \hat{d}_e(t) = {B_d}^{+}LC\Delta z(t) \\ \hat{d}_e(t) = d_e(t) - \Delta d(t) \end{cases} \tag{5}$$

where $\Delta z(t)$ is the difference between $z(t)$ and $\hat{z}(t)$, ${B_d}^{+}$ is the pseudo inverse matrix of B_d given by the following equation.

$${B_d}^{+} = \left({B_d}^{T}B_d\right)^{-1}{B_d}^{T} \tag{6}$$

For a more detailed discussion of the methodology, refer to [3].

3. Numerical Model

Table 1 shows the properties of the base-isolated building modeled as an 11-degree-of-freedom (DOF) system shown in Figure 1(a). The wind forces in the analysis were taken from a wind-tunnel experiment with a 500-year return period in the along-wind direction with design wind velocity of 63.8 m/s. The sensor configurations analyzed are shown in Table 2, with the goal of increasing the number of accelerometers while keeping the locations distributed across the building. Except for the S6_11

Table 1. Properties of the 11-DOF model

	Upper structure	Isolation layer
Natural period	$T_u = 2.0$ s	$T_b = 4.0$ s
Density	$\rho_u = 1715$ N/m^3	$\rho_b = 2551$ kg/m^2
Height	$H = 100$ m	
Area	$A = 625$ m^2	$A = 625$ m^2
Damping ratio	$\zeta_u = 2\,\%$	$\zeta_b = 20\,\%$
Yield shear coeff.		$\alpha_{by} = 0.03$
Yield deformation		$x_{by} = 3$ cm

model, where velocity responses in all DOFs are assumed to be known for an accurate comparison, all other models rely on acceleration sensors. Different observer gains are considered to account for errors introduced during response identification, which can be amplified when a high gain is assumed. The corresponding weighing value Q_2 for the observer gains are as follows: Low (10^4), Mid (10^6), and High (10^{16}).

Table 2. Sensor configurations

Model name	Number of sensors	Sensor locations
S1_04	4	BF, 1, 5, 10
S2_05	5	BF, 1, 3, 5, 10
S3_06	6	BF, 1, 3, 5, 7, 10
S4_07	7	BF, 1, 2, 3, 5, 7, 10
S5_10	10	BF, 1, 2, 3, 4, 5, 6, 7, 8, 10
S6_11	11	All DOFs (velocity sensors)

4. Results

Figures 2 and 3 show the results of the response identification. Interpolating the acceleration for stories without sensors resulted in a maximum error of approximately 25%, with the along-wind direction being less accurate than the across-wind direction (Figure 2). For the velocity response obtained through integration (Figure 3), cases with fewer sensors generally followed the acceleration data trend. However, regardless of the number of sensors, the isolation story exhibited significant errors in velocity estimation due to integration, as observed in models S3_06, S4_07, and S5_10.

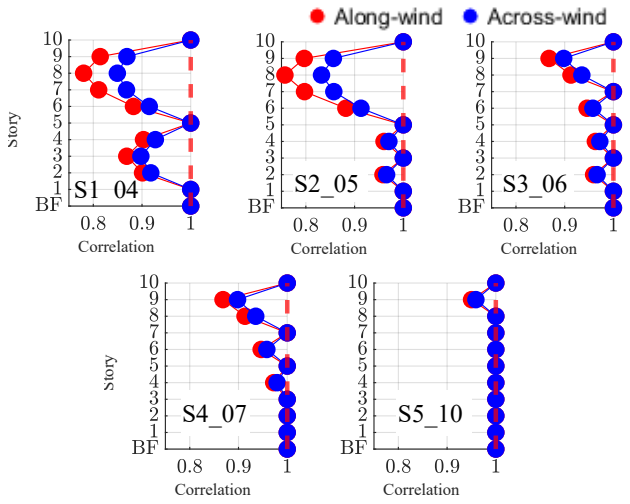

Figure 1. Accuracy of interpolated acceleration response

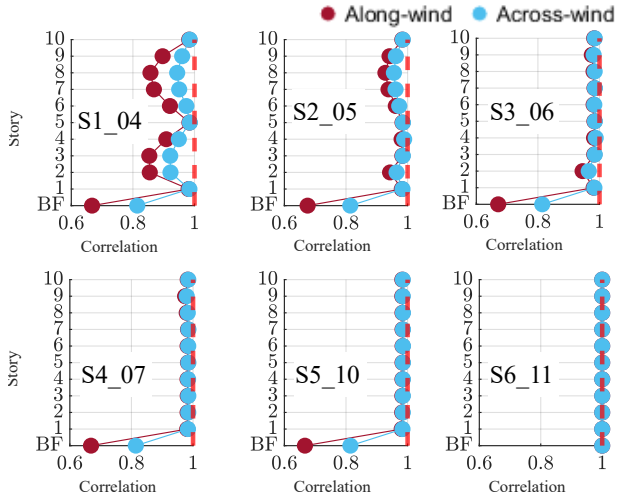

Figure 2. Accuracy of velocity response.

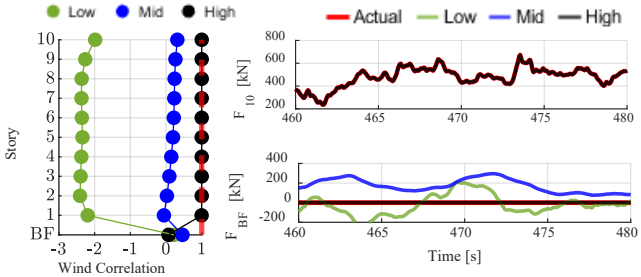

Figure 3. Wind force estimates (Model S6_11, along-wind).

Based on the response identification results, the following wind force time-histories were obtained. As expected, a high observer gain provided accurate wind estimates in both directions for the model with complete response data (see Figure 3). With only four sensors, a low observer gain was effective for the across-wind direction, whereas in the along-wind direction, it captured the fluctuating component but failed to estimate the mean component. For models with six or seven sensors, the mid observer gain yielded the highest accuracy. Additionally, for the lower stories, using a low observer gain improved the estimates in the across-wind direction but had limited effectiveness in the along-wind direction.

5. Conclusion

The results demonstrated that with appropriate adjustment of observer gains, the EID-NS method could accurately estimate the across-wind direction under conditions of limited sensors but encountered difficulties in estimating the mean component of the along-wind direction.

References:

[1] She, J. H., Fang, M., Ohyama, Y., Hashimoto, H., & Wu, M. (2008). Improving disturbance-rejection performance based on an equivalent-input-disturbance approach. IEEE Transactions on Industrial Electronics, 55(1), 380-389.

[2] Miyamoto, K., Sato, D., She, J., Chen, Y., & Nakano, S. (2022, July). Wind-load estimation with equivalent-input-disturbance approach. In *2022 IEEE/ASME International Conference on Advanced Intelligent Mechatronics (AIM)* (pp. 921-925). IEEE.

[3] Soriano RDA, Sato D, Miyamoto K, Chen Y, She J. Wind force estimation on a nonlinear seismic-isolated building by equivalent-input-disturbance method. *Journal of Vibration and Control*. 2025;0(0).

*1 東京科学大学
*2 清水建設株式会社 技術研究所
*3 東京工科大学　教授・博士（工学）

*1 Institute of Science Tokyo
*2 Institute of Technology, Shimizu Corporation
*3 Tokyo Univ. of Technology